

USABILITY STUDY TO QUALIFY A MAINTENANCE ROBOTIC SYSTEM FOR LARGE SCALE EXPERIMENTAL FACILITY

J. Y. Zhang^{†,1,3}, J. X. Chen², L. Kang¹, R. H. Liu², J. B. Yu²

¹Institute of High Energy Physics, Chinese Academy of Sciences, Beijing, China

²Spallation Neutron Source Science Center, Dongguan, China

³University of Chinese Academy of Sciences, Beijing, China

Abstract

The primary stripper foil device is one of the most critical devices of The China Spallation Neutron Source Project Phase-II (CSNS-II), which requires regular foil replacement maintenance to ensure its stable operation. To mitigate the potential hazards posed to workers by prolonged exposure to high levels of radiation, a maintenance robotic system has been developed to perform repetitive and precise foil changing task. The proposed framework encompasses various aspects of the robotic system, including hardware structure, target detection, manipulator kinematics design, and system construction. The correctness and efficiency of the system are demonstrated through simulations carried out using ROS Moveit! and GAZEBO.

INTRODUCTION

Nowadays, the role of robotics in industrial and scientific applications is growing exponentially, one of which is the usage of maintenance robotic systems in large experimental facilities such as Synchrotron Radiation Equipment and Instrumentation [1].

The China Spallation Neutron Source Project Phase-II (CSNS-II) poses ongoing challenges in terms of both its upgrade and remodelling. The primary stripper foil device is one of the most critical devices of CSNS-II, which undergoes significant changes due to the increased beam injection energy from 80 MeV to 300 MeV, as well as the radiation dose in the injection zone is expected to be further amplified (see Table 1). During the maintenance process, the foil components that are being exchanged need to be placed in radiation shielding containers until the radiation dose has decayed to a safe level before new foils can be installed.

Table 1: Downtime Dose Statistics

Shut-down Time	Proton-Induced Dose Rate	Dose Rate in 1 W/m Mode	Total Dose Rate
0 s	0.5 mSv/h	2.2 mSv/h	2.7 mSv/h
1 h	0.3 mSv/h	1.3 mSv/h	1.6 mSv/h
1 day	0.23 mSv/h	1.0 mSv/h	1.23 mSv/h
1 week	0.18 mSv/h	0.77 mSv/h	0.95 mSv/h
1 month	0.13 mSv/h	0.55 mSv/h	0.68 mSv/h

From the maintenance work described above, this paper presents a usability study that aims to evaluate a

maintenance robotic system for large-scale experimental facilities.

The findings of this study will contribute to the development of robust and reliable robotic system, which would emerge as viable industrial solutions to replace humans in executing construction tasks that are safe, efficient, and precise.

SYSTEM FRAMEWORK

The overall framework of the robotic system is depicted in Fig. 1, which consists of a vision and image processing system, a ROS operating system, a hardware system, and a host computer system.

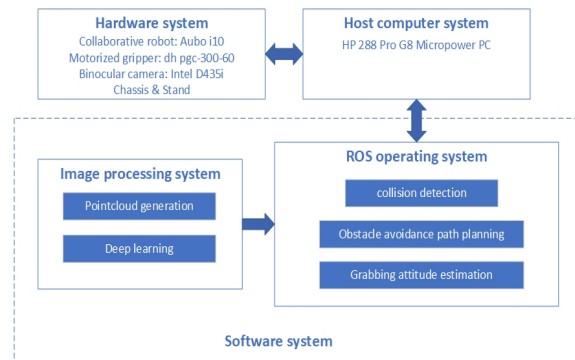


Figure 1: Robotic system framework.

Leveraging the Robot Operating System (ROS) platform, the proposed robotic system exhibits the capability to successfully execute target recognition and motion planning tasks for a 6-degree-of-freedom tandem robotic arm, as well as the ability to transition to a solid robot configuration. The system workflow diagram is illustrated in Fig. 2.

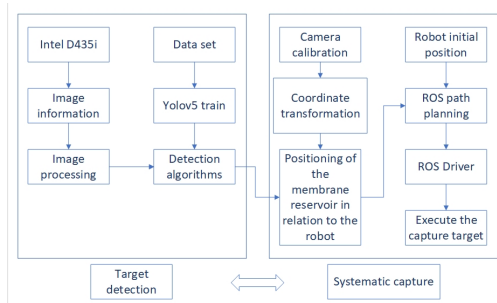


Figure 2: System workflow diagram.

Hardware Component Design

The entire system is installed in the CSNS Experiment II Testbed (see Fig. 3). Considering the workspace and

[†] zhangjingyu@ihep.ac.cn

Content from this work may be used under the terms of the CC-BY-4.0 licence (© 2023). Any distribution of this work must maintain attribution to the author(s), title of the work, publisher, and DOI

payload requirements, the AUBO-i10 arm with a customized fingertip end effector DH-PGC-300-60 was selected. Furthermore, the robot base, which was designed according to the beam height specifications, underwent static and modal analyses conducted using ANSYS Workbench to ensure stability and reliability. In the design of the robot grasping system, the depth camera is fixed in the world coordinate system, thereby ensuring that image acquisition is independent of the motion of the robotic arm.



Figure 3: Hardware components.

SOFTWARE SYSTEM

The main control tasks of the robotic system involve motion planning for grasping and placing the target objects. ROS Moveit! is an integrated development platform that includes various functionalities such as motion planning, kinematic solving, 3D perception, and perception configuration. Consequently, both motion control and planning of the robotic system are carried out within the ROS framework.

Machine Visualization

YOLOv5 is presently one of the most extensively employed algorithms for object detection, which primary objective is to accurately and efficiently detect objects in both images and videos [2].

As shown in Fig. 4, the structure of the YOLOv5 model consists of four main parts. During training, the algorithm divides the input image into $N \times N$ grids and predicts the bounding boxes and classes of objects in each grid, while optimizing network parameters to improve detection accuracy and speed.

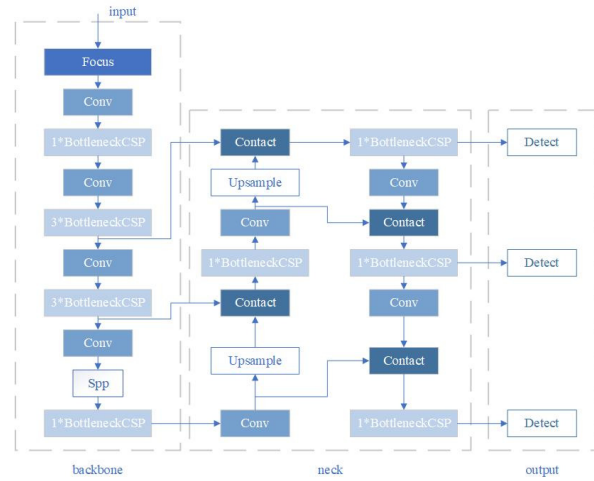


Figure 4: YOLOv5 network.

Coordinate Conversion

When predicting the grasp parameters of the target in the image, it is also necessary to perform coordinate transformations. Assuming the camera focal length is f , the image coordinate position is $P(x, y)$, and the camera position coordinate is $L_c(x_c, y_c, z_c)$. According to the camera imaging principle, Eq. (1) converts a two-dimensional pixel into a point in camera coordinate system.

$$\begin{bmatrix} x_c \\ y_c \\ z_c \\ 1 \end{bmatrix} = \begin{bmatrix} \frac{z_c}{f} & 0 & 0 \\ 0 & \frac{z_c}{f} & 0 \\ 0 & 0 & z_c \\ 0 & 0 & 1 \end{bmatrix} \begin{bmatrix} x \\ y \\ 1 \end{bmatrix}. \quad (1)$$

By further applying the pose transformation relationship between the camera coordinate system and the robot base coordinate system, based on Eq. (2), we can determine the optimal grasping point in the robot coordinate space $L_r(x_r, y_r, z_r)$.

$$\begin{bmatrix} u \\ v \\ 1 \end{bmatrix} = k \begin{bmatrix} R & T \\ 0 & 1 \end{bmatrix} \begin{bmatrix} x_r \\ y_r \\ z_r \end{bmatrix}. \quad (2)$$

Campaign Planning

The campaign planning mainly involves solving inverse kinematics and trajectory planning, as shown the workflow depicted in Fig. 5.

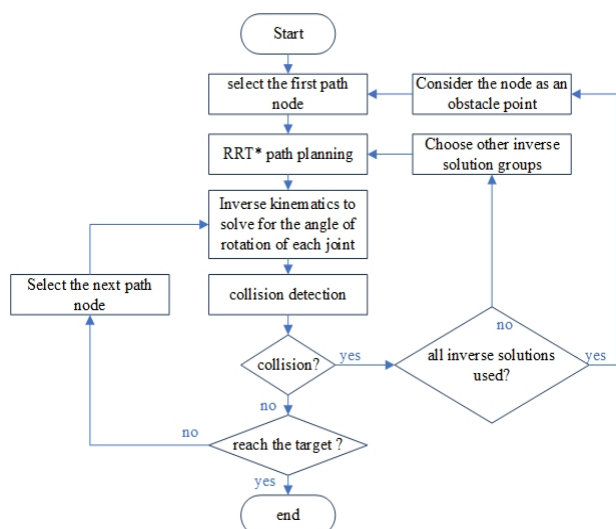


Figure 5: Trajectory planning.

The Bi-RRT* combines the benefits of RRT* in terms of finding optimal paths with the inherent efficiency and simplicity of RRT-Connect [3]. It is particularly useful in scenarios where an optimal and feasible path is desired in complex environments. The algorithm explores the configuration space from both the start and goal nodes simultaneously, aiming to find a feasible path connecting them.

Random 3D Scene Construction with Path Search Results, as shown in Fig. 6, the improved algorithm reduces search time and explored states (see Table 2).

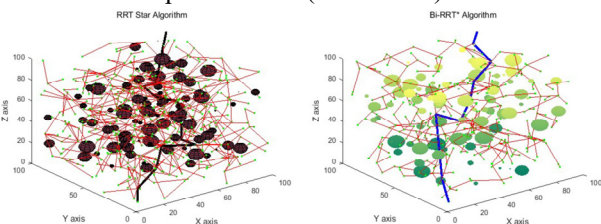


Figure 6: RRT* search result (right) and Bi-RRT* search result (left).

Table 2: Algorithm Comparison

Algorithm	Average Running Time	Average Explored States	Average State in Path
Bi-RRT*	1.91 s	4000	12.5
RRT*	0.12 s	159.5	10.5

EXPERIMENTS

Machine Visualization

The original dataset was created by capturing RGB images at different tilt angles and heights. To improve the generalization capability, the dataset of 300 samples was randomly divided into a training set (80 %) and a test set (20 %), using data augmentation techniques such as random rotation and brightness adjustment. In addition, the Labellmg annotation tool has been applied to annotate the outer bounding rectangle and assign class labels.

The training and testing of the model were conducted on a system with Windows 11 operating system, utilizing the PyTorch 2.0.1 deep learning framework, implemented in Python 3.9.

During the model training process, a batch size of 4 samples was used, with an initial learning rate of 0.01. After 100 iterations, The training and testing sample results are shown in Fig. 7, demonstrating successful target localization and recognition of the foil components.

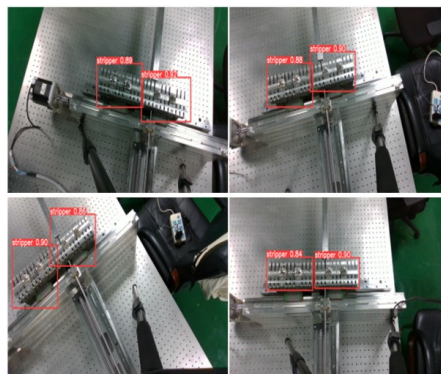


Figure 7: Testing set detection results.

Gazebo

Finally, the MoveIt! module is used to import the robot system and configure the grasp environment. The Move_group core node is then employed to establish communication between various software modules, enabling the simulation of arm grasping in the Gazebo environment (see Fig. 8).

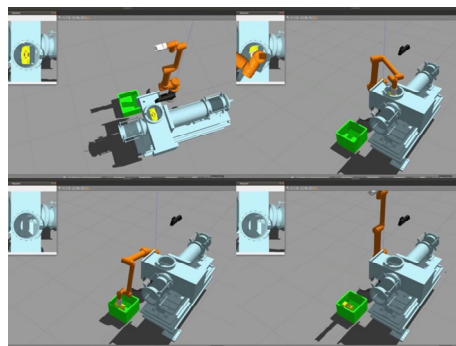


Figure 8: Simulation grasping results.

CONCLUSION

In conclusion, we have developed a grasping robotic system based on YOLOv5, which experiments in the simulated environment have demonstrated the effectiveness and feasibility of the system. This system holds great potential for a wide range of applications, as well as performs various maintenance tasks by equipping different end effectors.

Further improvements can be made to enhance the system's performance and adaptability, such as integrating more advanced object detection algorithms and optimizing the grasping mechanism. The next step will involve conducting real-world experiments based on the results obtained from object detection.

Overall, our work presents a new solution for the routine maintenance of gas pedal installations.

REFERENCES

- [1] M. Di Castro, M. Ferre, and A. Masi, "CERNTAURO: A Modular Architecture for Robotic Inspection and Telemanipulation in Harsh and Semi-Structured Environments," *IEEE Access*, vol. 6, pp. 37506-37522, 2018. doi:10.1109/access.2018.2849572
- [2] Y. Shao, D. Zhang, H. Chu, X. Zhang, and Y. Rao, "A Review of YOLO Object Detection Based on Deep Learning," *Journal of Electronics & Information Technology*, vol. 44, no. 10, pp. 3697-3708, Oct 2022. doi:10.11999/jeit210790
- [3] S. Karaman and E. Frazzoli, "Sampling-based algorithms for optimal motion planning," *Int. J. Rob. Res.*, vol. 30, no. 7, pp. 846-894, Jun 2011. doi:10.1177/0278364911406761